



# ThnL, a B<sub>12</sub>-dependent radical S-adenosylmethionine enzyme, catalyzes thioether bond formation in carbapenem biosynthesis

Erica K. Sinner<sup>a</sup>, Rongfeng Li<sup>a</sup>, Daniel R. Marous<sup>a,1</sup>, and Craig A. Townsend<sup>a,2</sup>

Edited by Mohammad Seyedsayamdost, Princeton University, Princeton, NJ; received April 13, 2022; accepted July 19, 2022 by Editorial Board Member Stephen J. Benkovic

Complex carbapenems are important clinical antibiotics used to treat recalcitrant infections. Their biosynthetic gene clusters contain three essential B<sub>12</sub>-dependent radical S-adenosylmethionine (rSAM) enzymes. The majority of characterized enzymes in this subfamily catalyze methyl transfer, but only one is required to sequentially install all methionine-derived carbons in complex carbapenems. Therefore, it is probable that the other two rSAM enzymes have noncanonical functions. Through a series of fermentation and in vitro experiments, we show that ThnL uses radical SAM chemistry to catalyze thioether bond formation between C2 of a carbapenam precursor and pantetheine, uniting initial bicycle assembly common to all carbapenems with later tailoring events unique to complex carbapenems. ThnL also catalyzes reversible thiol/disulfide redox on pantetheine. Neither of these functions has been observed previously in a B<sub>12</sub>-dependent radical SAM enzyme. ThnL expands the known activity of this subclass of enzymes beyond carbon-carbon bond formation or rearrangement. It is also the only radical SAM enzyme currently known to catalyze carbon-sulfur bond formation with only an rSAM Fe-S cluster and no additional auxiliary clusters.

B<sub>12</sub>-dependent radical SAM | carbapenam | antibiotic | thioether

Carbapenems are potent, broad-spectrum β-lactam antibiotics. They are used clinically for multidrug-resistant and hospital-acquired infections that cannot be treated by most other classes of antibiotics (1). Carbapenems are stable to many common β-lactamases, which confer bacterial resistance to other classes of β-lactam antibiotics (e.g., penicillins and cephalosporins) (2). Thus, they are a vital component of the current clinical response to antibiotic-resistant infections (3). Naturally occurring carbapenems can be divided into two subclasses: “simple” and “complex.” The simple carbapenam ((5*R*)-carbapenam-3-carboxylic acid, **1**) is produced by species of *Pectobacterium* (formerly *Erwinia*) and *Serratia*, and is composed of a bicyclic carbapenam core appended only by a C3 carboxylic acid (4). The complex carbapenems, which are more structurally diverse, are produced by the evolutionarily distant *Streptomyces* (5). Complex carbapenems share a core structure with the simple carbapenam, but are additionally functionalized at C2 and C6, as exemplified by the paradigm complex carbapenam, thienamycin (**2**). As shown in Fig. 1*A*, the enzymes responsible for the first two biosynthetic steps to construct the carbapenam bicycle **3** are homologous (in sequence and function) in simple and complex carbapenam biosynthetic gene clusters (BGCs) (6). The carbapenam initially formed by CarB/ThnE and CarA/ThnM is antibiotically inert due to its stereochemistry at C5. In the case of the simple carbapenam, the biosynthesis of the active antibiotic is completed by a single enzyme, CarC, which performs C5 inversion and C2–C3 desaturation to form **1** (7). The path to complex carbapenems diverges after bicycle formation, with functionalization at C2 and C6 preceding conversion to an active antibiotic. The C6 side chain contains a 1- to 3-carbon alkyl chain that is often hydroxylated, and can be further modified by oxidation and sulfation (8–11). The C2 side chain is attached to the carbapenam core by a carbon-sulfur bond, which tempers the high reactivity of the fused β-lactam ring, and ranges in length from a sulfonic acid (12, 13) to full-length pantetheine (PantSH) (14–16). However, the paradigm complex carbapenam, thienamycin (**2**), contains cysteamine at C2 (17), and many other carbapenam C2 side chains comprise its acetylated (10) and oxidized (8, 9) derivatives. Variation in both side chains gives rise to a structurally diverse family of *ca.* 50 carbapenam natural products (5). Representative members are shown in Fig. 1*B*.

The two complex carbapenam BGCs that have been thoroughly characterized both contain three Cobalamin (Cbl)-dependent radical S-adenosylmethionine (rSAM) enzymes (8, 18), all of which are essential for carbapenam production (8), and are, therefore, unlikely to have redundant functions. Most characterized Cbl-dependent rSAM enzymes catalyze methyl transfer (19, 20), and the complex carbapenam C6

## Significance

Structural diversity at C2, seen in both naturally occurring and clinically used synthetic carbapenems, is pivotal to their potency and spectrum of antibiotic activity. The stereoelectronic effect of the thioether at C2 is key to tuning the reactivity of the β-lactam ring for sufficient stability under physiologic conditions. Despite the importance of carbapenam antibiotics in the treatment of drug-resistant infections, the enzyme responsible for installation of the thioether has heretofore been unknown. We have found that ThnL catalyzes carbon-sulfur bond formation at C2, an unprecedented function for a B<sub>12</sub>-dependent radical SAM enzyme. It is likely that this function is not unique to ThnL, which could help unravel the biosynthetic pathways to other important sulfur-containing natural products.

Author affiliations: <sup>a</sup>Department of Chemistry, Johns Hopkins University, Baltimore, MD 21218

Author contributions: E.K.S., R.L., D.R.M., and C.A.T. designed research; E.K.S., R.L., and D.R.M. performed research; E.K.S., R.L., D.R.M., and C.A.T. analyzed data; and E.K.S. wrote the paper in discussion with all co-authors.

The authors declare no competing interest.

This article is a PNAS Direct Submission. M.S. is a guest editor invited by the Editorial Board.

Copyright © 2022 the Author(s). Published by PNAS. This article is distributed under Creative Commons Attribution-NonCommercial-NoDerivatives License 4.0 (CC BY-NC-ND).

<sup>1</sup>Present address: Department of Chemistry, Wittenberg University, Springfield, OH 45504.

<sup>2</sup>To whom correspondence may be addressed. Email: ctownsend@jhu.edu.

This article contains supporting information online at <http://www.pnas.org/lookup/suppl/doi:10.1073/pnas.2206494119/-DCSupplemental>.

Published August 15, 2022.

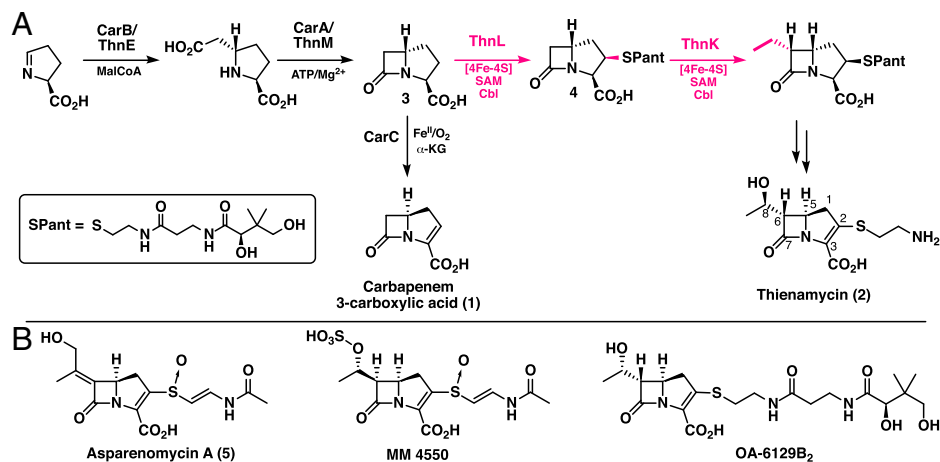


**Fig. 1.** (A) Biosynthetic pathways toward simple and complex carbapenems. Steps catalyzed by Cbl-dependent rSAM enzymes are shown in magenta. (B) Other representative complex carbapenems.

alkyl chain is known to be methionine derived (21). However, irrespective of length, the C6 alkyl chain is constructed by a single Cbl-dependent rSAM methylase. Two of these sequential methylases have been characterized in detail, namely, ThnK (22) and TokK (23–25), which are involved in the biosynthesis of thienamycin (2) and asparenomycin (5), respectively. This finding rendered it probable that the other two Cbl-dependent rSAM enzymes in thienamycin biosynthesis, ThnL and ThnP, have nonmethylase function. To our knowledge, the only biochemically characterized Cbl-dependent rSAM enzyme that is not a methylase is OxB, which catalyzes a ring-contracting rearrangement in oxetanocin biosynthesis (26, 27). BchE, which is involved in bacteriochlorophyll biosynthesis, is also unlikely to catalyze methyl transfer, but its function is incompletely understood (28, 29). With few remaining uncharacterized enzymes in complex carbapenem biosynthesis and the key C2–sulfur bond formation unassigned, we wondered if the catalytic potential of the Cbl-dependent rSAM platform could go beyond C–C bond formation. While the C2 cysteamine side chain of thienamycin is known to arise from the successive truncation of coenzyme A (CoA) (30), the identity of the enzyme responsible for C2 side chain installation has, until now, remained enigmatic. The experiments detailed below establish that ThnL catalyzes C2–PantSH thioether bond formation, transforming 3 into 4, which expands the repertoire of transformations carried out by this class of enzymes.

## Results and Discussion

**Identification of the ThnL Substrate.** Bioinformatic analysis of ThnL shows that it consists of an N-terminal B<sub>12</sub>-binding domain and a C-terminal rSAM domain containing a canonical CX<sub>2</sub>CX<sub>3</sub>C [4Fe–4S] cluster binding motif (SI Appendix, Fig. S1). Early studies indicated that ThnL acts early in the biosynthesis of thienamycin (18, 31). As has been detailed elsewhere (19), the study of Cbl-dependent rSAM enzymes has suffered from poor solubility upon heterologous expression, and ThnL was no exception. Early attempts to express and purify ThnL from *Escherichia coli* were unsuccessful. In addition, the thienamycin producer *Streptomyces cattleya*, is genetically intractable in our hands, making traditional knockout strategies difficult. Therefore, we developed a method using a heterologous *Streptomyces* host to precisely determine the position of ThnL in the biosynthetic pathway. The genes responsible for initial bicycle formation, namely, *thnE* and *thnM*, were first integrated into

the genome of *Streptomyces lividans* TK24 (32) to produce the TK24-EM strain (SI Appendix, Figs. S2 and S3A). Fermentation of this strain produces the carbapenem intermediate 3. However, as 3 is unstable and difficult to detect in a complex mixture, a bioassay was developed, as described in Fig. 2A. We utilized the dual-functional enzyme CarC (7, 33) to convert 3 into the antibiotic-active carbapenem 1, which can be visualized as a zone of growth inhibition on *E. coli* supersensitive strain (ESS), which is especially susceptible to β-lactam antibiotics (Fig. 2B) (34). Once this approach was validated (SI Appendix, Fig. S3B), *thnL* was integrated into the TK24-EM strain to create a platform for simultaneous heterologous expression of ThnE, ThnM, and ThnL (TK24-EML; SI Appendix, Fig. S3C). Fermentation of this strain in the presence of hydroxycobalamin (OHCbl) followed by incubation with CarC and plating on ESS does not result in a zone of inhibition (Fig. 2), indicating that carbapenem 3 has been transformed by ThnL into a compound incompatible with catalysis by CarC. Attempts to detect the ThnL product in the medium were unsuccessful. Fermentation of TK24-EML without OHCbl followed by CarC treatment and plating on ESS results in a zone of inhibition, suggesting that ThnL catalysis is dependent on Cbl. To further validate this result, an analogous strain containing ThnE, ThnM, and ThnK was constructed (SI Appendix, Fig. S3C). ThnK catalyzes sequential methylations only on C2–PantSH-containing substrates and does not methylate carbapenem 3 (22). As expected, the TK24-EMK strain produced levels of 3 comparable to the TK24-EM strain regardless of OHCbl supplementation, as visualized by the bioassay (Fig. 2). Taken together, these experiments suggest that carbapenem 3 is the ThnL substrate, placing this enzyme after ThnE and ThnM in thienamycin biosynthesis, but before ThnK.

**Initial Purification and Characterization of ThnL.** Fortunately, it was at this juncture that Booker and colleagues (35) developed the Cbl import plasmid pBAD-Btu-CEDFB as a tool to aid in the soluble expression of Cbl-dependent rSAM enzymes in *E. coli*. Coexpression of this plasmid and pDB1282 (which encodes Fe–S cluster biogenesis genes) with pET29b-*thnL* in LB medium supplemented with OHCbl enables the overproduction of soluble ThnL. Notably, ThnL produced in the absence of pBAD-Btu-CEDFB is completely insoluble. A single immobilized metal affinity chromatography (IMAC) step yields ThnL in insufficient purity for further analysis, so a TEV protease cleavage site was inserted into the expression vector before

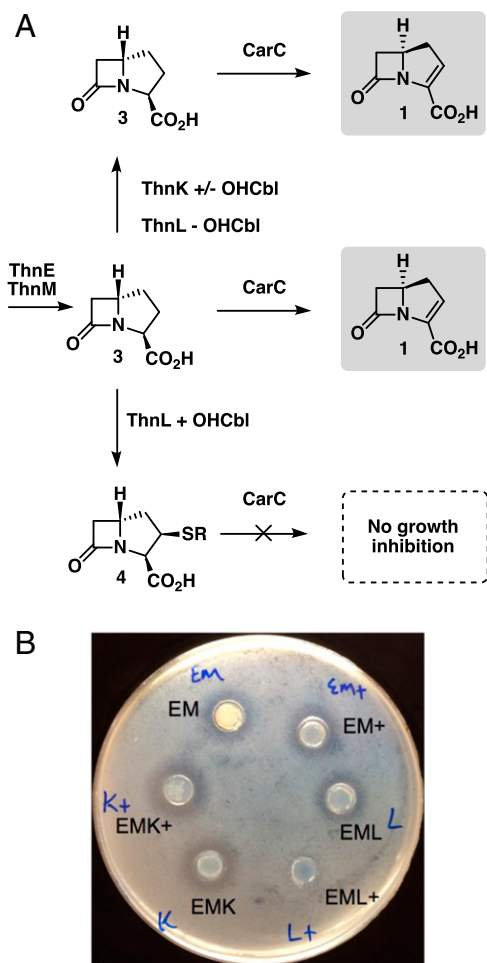


**Fig. 2.** Bioassay to detect **3** in the medium of *Streptomyces* fermentations through transformation to the antibiotically active **1** by CarC. (A) Schematic of assay setup. (B) Bioassay plate seeded with ESS. Letters indicate thn genes present, + indicates OHCbl supplementation. When ThnL and OHCbl are present, **3** is transformed into **4**, which is incompatible with CarC.

the C-terminal His<sub>6</sub>-tag (*SI Appendix*, Fig. S4). A second IMAC step after the affinity tag is cleaved gives 90 to 95% pure protein (Fig. 3A) at 0.2 mg/L to 0.3 mg/L of expression culture. ThnL was anaerobically purified using methods similar to those developed for TokK and ThnK (25). Protein concentration was determined by the Bradford assay with a correction factor of 1.21 as determined by amino acid analysis. The UV-visible spectrum of purified ThnL shown in Fig. 3B displays a 420-nm shoulder, which signifies the presence of a bound [4Fe-4S] cluster. Quantitation of iron and sulfide using established colorimetric methods (36–38) shows 0.4 irons and 0.3 sulfides per polypeptide, indicating less than 10% [4Fe-4S] cluster occupancy in purified ThnL. Chemical reconstitution with FeCl<sub>3</sub> and Na<sub>2</sub>S (as described in ref. 25) results in 1.2 irons and 0.4 sulfides per polypeptide, but does not increase enzyme activity. To assess whether ThnL binds Cbl, the protein was heated with potassium cyanide. This method liberates any bound Cbl as dicyanocobalamin, which can be quantitated by absorbance at 367 nm (39), and shows that purified ThnL contains Cbl at 80 to 90% occupancy, which is not increased upon reconstitution with OHCbl (Fig. 3C). Further analysis by tandem ultraperformance liquid chromatography/high-resolution mass spectrometry (UPLC-HRMS) and comparison to standards shows that ThnL contains mostly OHCbl, with a minor amount of AdoCbl, and no MeCbl (Fig. 3D).

**ThnL Is Specific for PantSH.** Purified ThnL was assayed for activity with carbapenam substrate **3** and potential thiol donors, as shown in Fig. 3E. CoASH, phosphopantetheine (PPantSH), PantSH, and *N*-acetyl cysteamine (SNAC) were chosen to represent the pool of thiols available based on the CoA truncating enzymes found in the thienamycin BGC (30). While cysteamine is the C2 thioether found in thienamycin, the nucleophilicity of the primary amine hastens the degradation of the already unstable carbapenam **3**, and, therefore, SNAC was used in its place. In addition to **3** and a thiol donor, each enzymatic reaction contained ThnL, SAM, methyl viologen, and reduced nicotinamide-adenine dinucleotide phosphate (NADPH) in HEPES buffer (pH 7.5). These conditions mirrored those that were successful with ThnK, and therefore were used as a starting point. After incubation for 1 h, the assay mixtures were passed through Amicon ultrafiltration devices, and the filtrate was assayed for product formation by UPLC-HRMS. Extracted-ion chromatograms (EICs) were generated for each expected thioether product (Fig. 3E). Assays containing PantSH as the thiol donor showed accumulation of a product that matches the mass of pantetheinylated carbapenam **4**. No product was found in assays with CoA or PPantSH, while a small amount of putative product was observed with SNAC. These data suggest that ThnL is a relatively selective biosynthetic enzyme that installs a C2 PantSH thioether on the ThnM product **3**. Comparison of the ThnL product with synthetic standards shows that ThnL catalysis is stereospecific and yields the pantetheinylated carbapenam **4** having the *R* configuration (*exo*) at C2 (Fig. 3F and *SI Appendix*, Fig. S5). The installation of PantSH onto carbapenam **3** suggests that thioether bond formation by ThnL is the only enzymatic step between bicycle formation by ThnM and C6 alkylation by ThnK. This conclusion is in accord with the fact that ThnK methylation is more efficient with the 2*R* diastereomer than its *endo* 2*S* counterpart (22).

**ThnL Is an rSAM Enzyme.** In order to further characterize ThnL reaction, optimized conditions were desirable. Replacement of the methyl viologen/NADPH reducing system with titanium(III) citrate (TiCitrate) improved product output by approximately sixfold in a 1-h fixed-time assay (*SI Appendix*, Fig. S6) and was therefore used for all subsequent experiments. Additionally, it was found that the disulfide pantetheine, hereafter referred to as (PantS)<sub>2</sub>, could be used in place of PantSH. A series of control reactions, each lacking a single component of the assay mixture, was carried out (Fig. 3F). The data show that ThnL, SAM, a reductant, carbapenam **3**, and (PantS)<sub>2</sub> are all required for product formation. To validate that ThnL uses rSAM chemistry to accomplish thioether bond formation, site-directed mutagenesis was used to replace each of the three cysteines in the CX<sub>2</sub>CX<sub>3</sub>C motif with alanine. This variant, annotated as AX<sub>2</sub>AX<sub>3</sub>A, is unable to form product, as shown in Fig. 3F. In addition, 5'-deoxyadenosine (5'-dAH) is produced in ThnL assays, which is a hallmark of the reductive cleavage of SAM by a [4Fe-4S] cluster. As shown in Fig. 3J, the production of 5'-dAH is dependent on carbapenam **3**, SAM, and TiCitrate. It is observed only when wild-type ThnL is used, and is not formed in the absence of enzyme or with the AX<sub>2</sub>AX<sub>3</sub>A variant (Fig. 3J). Interestingly, 5'-dAH is produced in the absence of (PantS)<sub>2</sub>, possibly indicating that it is involved in the activation of the carbapenam substrate. Production of 5'-dAH is superstoichiometric to product **4** by more than 10-fold, suggesting an inefficiency somewhere in the catalytic cycle of ThnL. Unlike most characterized Cbl-dependent rSAM enzymes, ThnL does not produce

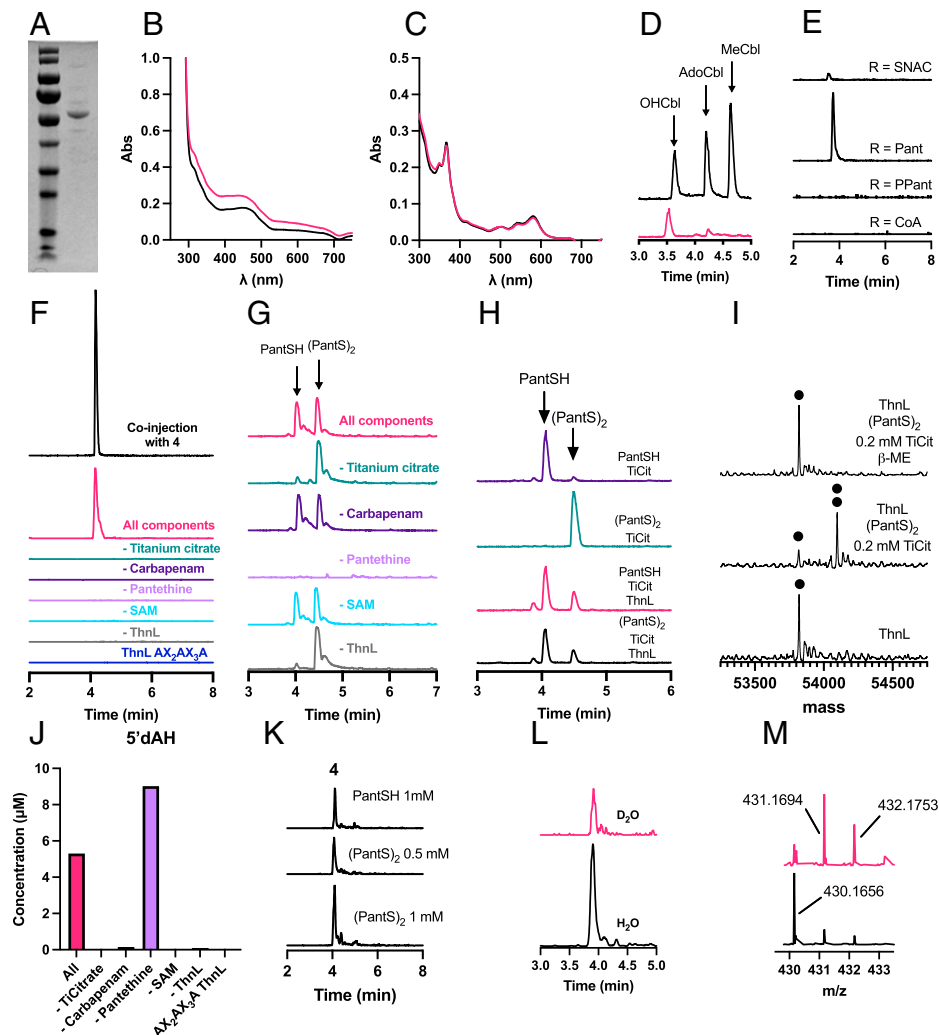


**Fig. 3.** Characterization of ThnL in vitro. (A) Sodium dodecyl sulfate polyacrylamide gel electrophoresis analysis of ThnL. Lane 1: PageRuler Protein Ladder; lane 2: purified ThnL. (B) UV-visible spectrum of ThnL (15  $\mu$ M) before (black) and after (magenta) chemical reconstitution with  $\text{FeCl}_3$ ,  $\text{Na}_2\text{S}$ , and  $\text{OHcbl}$ . (C) UV-visible spectrum of ThnL (10  $\mu$ M) treated with KCN before (black) and after (magenta) chemical reconstitution. (D) UPLC-HRMS analysis (total ion chromatograms, TICs) of Cbl bound to ThnL. Commercially available standards are shown in black, and Cbl liberated from ThnL is shown in magenta. (E) Negative-mode EICs of expected thioether product from activity assays with ThnL, **3**, and R-SH, where R is as indicated for each trace (from top to bottom,  $m/z = 271.08 \pm 0.03$ ,  $430.17 \pm 0.03$ ,  $510.13 \pm 0.03$ , and  $919.15 \pm 0.03$ ). (F) Negative-mode EICs of **4** ( $m/z = 430.17 \pm 0.03$ ) in assays; (-) indicates controls lacking that component. (G) TICs from activity assays with ThnL; major peaks are PantSH and  $(\text{PantS})_2$  as indicated. (H) TICs from PantSH redox assays. Components included in each assay are indicated next to the corresponding trace. (I) Intact-protein mass spectra of ThnL incubated with the components indicated next to each trace; • denotes apo protein (53,819 Da); •• denotes ThnL-Pant (54,095 Da). (J) Concentration of 5'-dAH formed in activity assays with 100  $\mu$ M ThnL. Product **4** (0.061  $\mu$ M) is formed only when all components are present. (K) Negative-mode EICs of **4** ( $m/z = 430.17 \pm 0.03$ ) in activity assays with the PantSH donor identity and concentration indicated on each trace. (L) EICs of product formed in activity assays in heavy and light water ( $m/z = 431.17 \pm 0.03$  and  $430.17 \pm 0.03$ , respectively). (M) Negative-mode ESI mass spectra of product formed in heavy and light water.

S-adenosyl homocysteine (SAH) during catalysis (*SI Appendix*, Fig. S7). As SAH is the product of Cbl methylation by SAM, this observation confirms that MeCbl is not an intermediate and that ThnL is not a methyl transferase. The role of Cbl in ThnL catalysis remains unclear, as the enzyme cannot be purified in the absence of intracellular Cbl as facilitated by pBAD-BtuCEDFB. However, the *Streptomyces* expression experiments outlined above indicate that Cbl is required for ThnL activity.

**ThnL Catalyzes Reversible Thiol/Disulfide Redox.** As mentioned above, ThnL is capable of thioether bond formation when incubated with either PantSH or  $(\text{PantS})_2$ . Surprisingly, when ThnL was assayed with  $(\text{PantS})_2$ , the formation of PantSH was observed (Fig. 3G). Disulfide reduction is dependent on the presence of both TiCitrate and ThnL, leading to the conclusion that TiCitrate alone is not sufficient for the reduction, but rather that it is an enzyme-dependent process.

However, SAM and carbapenam **3** are not required for disulfide reduction to be observed. Additionally, the thiols used in the initial side chain donor screen were stored aerobically, and were therefore contaminated with a small amount of  $(\text{PantS})_2$  formed by oxidation in air. Therefore, a mixture of PantSH and  $(\text{PantS})_2$  had been present in all assays up to this point. To clarify whether the thiol or disulfide was the catalytically competent PantSH donor, we prepared PantSH by reduction of  $(\text{PantS})_2$  with excess  $\text{NaBH}_4$  in aqueous solution under an anaerobic atmosphere. After neutralization with acetic acid, the solution was used directly in assays with freshly purified ThnL. As shown in Fig. 3K, fixed-time assays containing 1 mM PantSH produced a comparable amount of product **4** to that formed in assays with 0.5 mM  $(\text{PantS})_2$ . When the concentration of  $(\text{PantS})_2$  was doubled to 1 mM, product formation correspondingly increased. These results indicate that product formation is dependent on the amount of PantSH monomer,

regardless of oxidation state. Additionally, in assays with PantSH, we observed enzyme-dependent oxidation to (PantS)<sub>2</sub>, with the resulting ratio of thiol to disulfide very similar to that in assays with (PantS)<sub>2</sub> (Fig. 3H). These data suggest thiol/disulfide redox catalyzed by ThnL is reversible, and that the equilibrium reached under our reducing assay conditions is skewed toward the thiol form.

To further investigate this surprising redox function of ThnL, we turned to intact protein UPLC-HRMS (Fig. 3I and SI Appendix, Fig. S8). Because of the denaturing conditions of the chromatography step, ThnL is observed in *apo* form, without any bound metallofactors. When ThnL is incubated with (PantS)<sub>2</sub> and a limiting amount of TiCitrate, the mass shifts by 276 Da, corresponding to ThnL + PantSH – 2H, indicating the formation of a covalent ThnL–Pant adduct. Despite (PantS)<sub>2</sub> being present at 10× the concentration of ThnL, only a single adduct is observed, minimizing the likelihood of non-specific binding. When the ThnL–Pant adduct is exposed to β-mercaptoethanol, the adduct is lost, and ThnL is again observed in the *apo* form, demonstrating that formation of the adduct is reversible and susceptible to reduction by free thiol in the medium. Attempts to localize the adduct by trypsinolysis were unsuccessful. There are only three cysteine residues outside of the CX2CX3C motif, namely, Cys21, Cys22, and Cys391. Site-directed mutagenesis to replace each cysteine with alanine was carried out, but the resulting variants suffered from extremely low expression and cofactor occupancy, prohibiting conclusive analysis of the effects of the amino acid substitutions. Further, the practical limitations encountered during the study of ThnL currently preclude firm determination of the importance of this covalent adduct in either thiol/disulfide redox or thioether bond formation catalyzed by ThnL.

**Mechanistic Insight into ThnL Catalysis.** Since the activity of ThnL is unprecedented for a Cbl-dependent rSAM enzyme, we wanted to probe its mechanism. As stated above, the dependence of 5'-dAH production on the presence of carbapenam **3** but not on (PantS)<sub>2</sub> suggests that rSAM chemistry activates C2 of **3** either directly or indirectly. Conceivably, direct activation at C2 by hydrogen abstraction could be followed by radical coupling to (PantS)<sub>2</sub> or a ThnL–Pant adduct (Fig. 4A). Alternatively, C2 could be transformed into an activated electrophile through the intermediacy of a carbapenam species, which could accept a thiol/thiolate nucleophile. This mode of reactivity mirrors the way we prepare thioether **4** synthetically, and so is intuitively appealing. As shown in Fig. 4B, formation of a carbapenam could occur through hydrogen abstraction at C3, to form a classical captodative (push–pull) stabilized radical (40, 41), which could then undergo a one-electron oxidation to form a C3 cation. Single-electron transfer has been proposed analogously to Cbl or the Fe–S cluster in OxsB, another Cbl-dependent rSAM enzyme that is not a methylase (26, 27, 42). This cation would be further stabilized as an acyliminium ion as shown in Fig. 4B, which would readily eliminate a proton to give the carbapenam. The reaction would be completed by the conjugate addition of PantS<sup>–</sup>. In order to differentiate between these two possible mechanisms, ThnL assays were carried out in D<sub>2</sub>O. Since TiCitrate is prepared from TiCl<sub>3</sub> in 30% HCl, we used methyl viologen/NADPH as a reducing system to minimize the number of protons present. As shown in Fig. 3L, a product is formed at the same retention time in both heavy and light water. However, the negative-mode electrospray ionization (ESI) mass spectrum of product formed in D<sub>2</sub>O displays a shifted isotopic envelope when compared to control reactions

run in H<sub>2</sub>O (Fig. 3M). The [M–H] peak is nearly abolished, while the major peak is increased by one mass unit, suggesting that deuterium is incorporated into the product. In addition, the [M–H]+2 peak is approximately threefold larger than would be predicted if it was due to natural abundance <sup>13</sup>C in the [M–H]+1 species. Therefore, while the major product contains only one deuterium, 20 to 30% of product formed has incorporated two deuterium atoms. This observation makes mechanistic pathway A unlikely to be the one used in ThnL catalysis and may elevate the possibility that pathway B is operative, as it requires protonation from the medium. However, the incorporation of more than one deuterium into a substantial fraction of the product prompted the further recognition that the through-conjugated acyliminium ion is acidic at C2 and prone to exchange in deuterated medium that could be competitive with enamide (carbapenam) formation and thiol(ate) addition to carbapenam **4**.

The unique circumstances of electron delocalization of both radical and ionic species at C3 led us to consider a third mechanistic possibility, as depicted in Fig. 4C. In this case, C2 hydrogen abstraction is followed by C3 deprotonation to form a resonance-stabilized radical anion (43, 44). Deuterium uptake at both C2 and C3 could be mediated by reversible anion formation. One resonance form of this species is nucleophilic at C2, which could capture an electrophilic form of PantSH, either as (PantS)<sub>2</sub> or a ThnL–Pant adduct. Following C–S bond formation, the resulting C3 radical would be reduced and protonated, which would account for deuterium incorporation. Alternatively, the resonance form with the radical at C2 could attack a PantSH disulfide, followed by protonation of the C3 anion. Whether by radical, nucleophilic, or electrophilic means, further work is needed to clarify the mechanism by which ThnL catalysis occurs.

**ThnL in the Context of the rSAM Superfamily.** While thioether bond formation is an unprecedented reaction for a Cbl-dependent rSAM enzyme, there are several well-known examples of C–S bonds formed by rSAM enzymes which do not contain Cbl (45). However, all C–S bond-forming rSAM enzymes apart from ThnL are unified by binding one or more auxiliary Fe–S clusters in addition to the rSAM cluster. The function of these auxiliary clusters is not well understood and likely varies from enzyme to enzyme. Biotin synthase (46, 47) and lipoyl synthase (48–50) have sacrificial auxiliary clusters that serve as the sulfur source for C–H sulfur insertion reactions at unactivated aliphatic positions. In the case of methylthiotransferases RimO (51) and MiaB (52), which transfer –SCH<sub>3</sub> to their substrates, the auxiliary cluster has long been thought to serve as a coordination site for the sulfur donor (53), but recent evidence suggests that the auxiliary cluster may be the source of sulfur in MiaB (54). A third type of C–S bond-forming rSAM enzymes are in the SPASM/twitch subfamily (55), which all contain one or two auxiliary Fe–S clusters. The SPASM/twitch enzymes that catalyze C–S bond formation make posttranslational cross-links between cysteine thiols and the peptide backbone in ribosomally synthesized and posttranslationally modified peptide scaffolds such as sactipeptides (56–58). The mechanisms of several of these thioether-forming SPASM/twitch enzymes have been investigated, including AlbA, SkfB, and RumMC2 (59–61). The roles played by the auxiliary clusters in these enzymes are not fully understood, but they have been suggested to aid in substrate binding and/or electron transfer (59, 62, 63). It is possible that

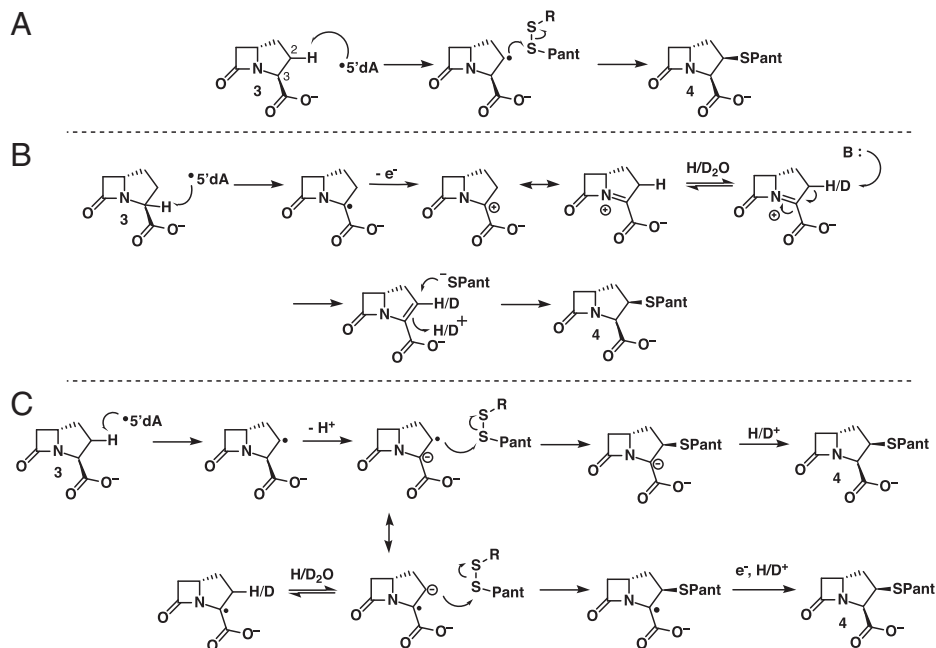


**Fig. 4.** Possible mechanisms of thioether bond formation by ThnL: (A) Radical coupling at C2, (B) formation of a C2-electrophilic carbapenem followed by nucleophilic addition of PantS<sup>-</sup>, and (C) radical anion formation followed by nucleophilic attack of C2 carbanion on a PantSH disulfide.

the observed ThnL–Pant adduct could similarly facilitate catalysis by proximity.

We have presented herein the initial characterization of ThnL, a Cbl-dependent rSAM enzyme that introduces the key C2–PantSH thioether in thienamycin biosynthesis. Therefore, we have established that construction of both the C2 and C6 carbapenem side chains is initiated by Cbl-dependent rSAM enzymes. These structural elaborations distinguish complex carbapenems from the simple carbapenem **1**, which is too hydrolytically unstable to be clinically useful. The chemical and physical properties engendered by these side chains impart the potency, spectrum of activity, and resistance to  $\beta$ -lactamases that set the carbapenems apart from other  $\beta$ -lactam antibiotics in the clinic (3, 5). In addition to catalyzing thioether formation, ThnL also has reversible thiol/disulfide redox activity. Both characterized functions of ThnL are unprecedented for the Cbl-dependent subclass of rSAM enzymes, expanding the known capabilities of the sophisticated combination of cofactors employed by these enzymes to include thioether bond formation beyond C–C bond formation. As there are thousands of uncharacterized Cbl-dependent rSAM enzymes, catalysis of thioether bonds is unlikely to be unique to ThnL. Continued study of this class of enzymes could be the key to understanding the biosynthesis of other important sulfur-containing natural products.

## Materials and Methods

**General Methods and Instrumentation.** General methods and instrumentation are described in *SI Appendix*.

**Construction of Strains for *Streptomyces* Experiments.** Experimental details can be found in *SI Appendix*.

**CarC Cell-Free Extract Assay.** CarC cell-free extract (CFE) was prepared as described in *SI Appendix*. The assay was done in 0.5- to 1-mL total volume, including 8 mM  $\alpha$ -ketoglutarate, 80  $\mu$ M ammonium iron(II) sulfate hexahydrate, 1 mM to 2 mM ascorbic acid, 62 to 63% (by vol) supernatant from *Streptomyces* fermentation culture, and 25% (by vol) CarC CFE. After mixing, reactions were run for 1 h to 1.5 h at 28 °C. Then, 200- $\mu$ L aliquots were plated on ESS.

**Overproduction of ThnL.** The pET29b/*thnL*-pBAD/*btuCEDFB*-pDB1282 strain (prepared as described in *SI Appendix*) was grown in the presence of kanamycin (50  $\mu$ g/mL), spectinomycin (50  $\mu$ g/mL), and ampicillin (100  $\mu$ g/mL) during all steps. Starter cultures grown in Luria-Bertani broth, standard stuff for growing cells (LB) medium (2  $\times$  100 mL) overnight at 37 °C were used to inoculate 6  $\times$  2.5 L of expression cultures in LB medium supplemented with 1.3  $\mu$ M hydroxocobalamin. These cultures were grown at 37 °C with 185 rpm shaking to optical density (OD) 0.35, and then pDB1282 and pBAD42-BtuCEDFB were induced with arabinose (1g/L), FeCl<sub>3</sub> (6.8 mg/L), and cysteine (24 mg/L). The cultures were grown to OD 0.8 and then cold shocked at 0 °C for 2 h. FeCl<sub>3</sub> and cysteine were added as before, along with isopropylthio- $\beta$ -galactoside (1 mM final concentration). The cultures were grown at 18 °C for an additional 20 h before harvesting by centrifugation at 4,000  $\times$  *g*. Cell paste was flash frozen in liquid N<sub>2</sub> and stored in liquid N<sub>2</sub> until use.

**Anaerobic Purification of ThnL.** In a Coy anaerobic chamber, cell paste (~50 g) from 15 L of culture grown as described above was resuspended in lysis buffer (10% glycerol, 300 mM KCl, 50 mM Hepes, 10 mM  $\beta$ -mercaptoethanol [BME], 5 mM imidazole, pH 7.5) to a final volume of 160 mL. Lysozyme (160 mg) was added, and the mixture was incubated on ice for 1 h before the cells were disrupted by sonication (60% amplitude, 9.9 s on/off, ~10 min). The lysate was placed in centrifuge tubes, sealed with vinyl tape, and clarified by centrifugation (35 min, 35,000  $\times$  *g*, 4 °C). After reentry into the anaerobic chamber, the supernatant was incubated with Clontech TALON metal affinity resin (6 mL 50% suspension, preequilibrated with lysis buffer) on ice for 30 min. The suspension was loaded onto a gravity column and washed with 10 mL to 20 mL of lysis buffer. The protein was then eluted with elution buffer (lysis buffer with 250 mM imidazole). The dark-colored elution fractions (~3 mL) were desalted on an Econo-Pac 10DG column (Bio-Rad) according to the manufacturer's instructions using desalting buffer (lysis buffer with no imidazole). The eluate was then incubated with TEV protease expressed from pRK793 (0.5 mg) (64) overnight on ice. Chemical reconstitution of iron and sulfide could be carried out simultaneously as described elsewhere (25). After cleavage and reconstitution, Clontech TALON metal affinity resin was added (4 mL 50% suspension, preequilibrated with desalting buffer) and incubated for 30 min on ice. The suspension was loaded onto a gravity column. The flow-through was collected, and the resin was washed with desalting buffer (4 mL). These fractions were combined and concentrated in a 10-kDa MWCO Amicon ultrafiltration device (MilliporeSigma) followed by buffer exchange using an Econo-Pac 10DG column into desalting buffer lacking BME so as to minimize interference in redox assays. The eluate was collected and concentrated to 0.5- to 1-mL volume, and protein concentration was measured using the

Bradford assay with a correction factor of 1.21 determined by amino acid analysis (University of California, Davis Molecular Structure Facility). Purified ThnL must be used directly in activity assays. Once BME is removed, the protein is active for ~8 h, after which product formation in activity assays diminishes to undetectable levels.

**Small-Molecule Activity Assays.** Assays were conducted at room temperature under an anaerobic atmosphere. Typical assays contained Hepes (100 mM, pH 7.5), KCl (200 mM), SAM (1 mM), freshly prepared titanium citrate (2 mM) (65), carbapenam **3** (1 mM), pantethine (1 mM), and ThnL (100  $\mu$ M). Other thiol donors were used in place of pantethine in various assays, and methyl viologen (1 mM) and NADPH (2 mM) were used to replace titanium citrate where indicated. After 1 h, a 20- $\mu$ L aliquot was diluted 5 $\times$  with water and filtered through a 10-kDa MWCO Amicon ultrafiltration device. The filtrate was analyzed by UPLC-HRMS with electrospray ionization in negative mode. Mobile phase was 0 min to 1 min 100% water, 1 min to 7.5 min gradient from 0 to 80% acetonitrile (ACN), 7.5 min to 8.4 min isocratic 80% ACN, and 8.4 min to 10 min 100% water. Flow rate was 0.3 mL/min.

**Intact Protein Analysis.** ThnL (100  $\mu$ M) was incubated with pantethine (1 mM) and titanium citrate (0.2 mM) for 1 h, followed by dilution to 5  $\mu$ M and centrifugation for 3 min at 15,000  $\times g$ . Samples were then analyzed by UPLC-HRMS. Mobile phase (containing 0.1% formic acid) was 0 min to 1 min 100% water, 1 min to 7.5 min gradient from 0 to 80% ACN, 7.5 min to 8.4 min isocratic 80% ACN, and 8.4 min to 12 min 100% water. Flow rate was 0.3 mL/min.

1. P. M. Hawkey, D. M. Livermore, Carbapenem antibiotics for serious infections. *BMJ* **344**, e3236 (2012).
2. R. A. Bonomo,  $\beta$ -Lactamases: A focus on current challenges. *Cold Spring Harb. Perspect. Med.* **7**, a025239 (2017).
3. K. M. Papp-Wallace, A. Endimiani, M. A. Taracila, R. A. Bonomo, Carbapenems: Past, present, and future. *Antimicrob. Agents Chemother.* **55**, 4943–4960 (2011).
4. W. L. Parker *et al.*, SQ 27,860, a simple carbapenem produced by species of *Serratia* and *Erwinia*. *J. Antibiot. (Tokyo)* **35**, 653–660 (1982).
5. C. A. Townsend, Convergent biosynthetic pathways to  $\beta$ -lactam antibiotics. *Curr. Opin. Chem. Biol.* **35**, 97–108 (2016).
6. M. J. Bodner *et al.*, Definition of the common and divergent steps in carbapenem  $\beta$ -lactam antibiotic biosynthesis. *ChemBioChem* **12**, 2159–2165 (2011).
7. R. Li, A. Stapon, J. T. Blanchfield, C. A. Townsend, Three unusual reactions mediate carbapenem and carbapenam biosynthesis. *J. Am. Chem. Soc.* **122**, 9296–9297 (2000).
8. R. Li, E. P. Lloyd, K. A. Moshos, C. A. Townsend, Identification and characterization of the carbapenem MM 4550 and its gene cluster in *Streptomyces argenteolus* ATCC 11009. *ChemBioChem* **15**, 320–331 (2014).
9. Y. Kawamura, Y. Yasuda, M. Mayama, K. Tanaka, Asparenomyins A, B and C, new carbapenem antibiotics. I. Taxonomic studies on the producing microorganisms. *J. Antibiot. (Tokyo)* **35**, 10–14 (1982).
10. T. Ohta, N. Sato, T. Kimura, S. Nozoe, K. Izawa, Chiro-specific synthesis of (+)-PS-5 from L-glutamic acid. *Tetrahedron Lett.* **29**, 4305–4308 (1988).
11. K. E. Wilson, A. J. Kempf, J. M. Liesch, B. H. Arison, Northienamycin and 8-*epi*-thienamycin, new carbapenems from *Streptomyces cattleya*. *J. Antibiot. (Tokyo)* **36**, 1109–1117 (1983).
12. N. Tsuji *et al.*, The structures of pluracidomyins, new carbapenem antibiotics. *J. Antibiot. (Tokyo)* **35**, 536–540 (1982).
13. N. Tsuji *et al.*, Pluracidomyin A2, a new carbapenem bearing a sulfinic acid, and other minor pluracidomyins. *J. Antibiot. (Tokyo)* **38**, 270–274 (1985).
14. T. Yoshioka *et al.*, Structures of OA-6129D and E, new carbapenam antibiotics. *J. Antibiot. (Tokyo)* **37**, 211–217 (1984).
15. T. Yoshioka *et al.*, Structures of OA-6129A, B1, B2 and C, new carbapenem antibiotics. *Tetrahedron Lett.* **23**, 5177–5180 (1982).
16. M. Okabe *et al.*, Studies on the OA-6129 group of antibiotics, new carbapenem compounds. I. Taxonomy, isolation and physical properties. *J. Antibiot. (Tokyo)* **35**, 1255–1263 (1982).
17. J. S. Kahan *et al.*, Thienamycin, a new  $\beta$ -lactam antibiotic. I. Discovery, taxonomy, isolation and physical properties. *J. Antibiot. (Tokyo)* **32**, 1–12 (1979).
18. L. E. Núñez, C. Méndez, A. F. Braña, G. Blanco, J. A. Salas, The biosynthetic gene cluster for the  $\beta$ -lactam carbapenem thienamycin in *Streptomyces cattleya*. *Chem. Biol.* **10**, 301–311 (2003).
19. E. K. Sinner, D. R. Marous, C. A. Townsend, Evolution of methods for the study of cobalamin-dependent radical SAM enzymes. *ACS Bio Med Chem Au* **2**, 4–10 (2022).
20. S. C. Wang, Cobalamin-dependent radical S-adenosyl-L-methionine enzymes in natural product biosynthesis. *Nat. Prod. Rep.* **35**, 707–720 (2018).
21. J. M. Williamson *et al.*, Biosynthesis of the  $\beta$ -lactam antibiotic, thienamycin, by *Streptomyces cattleya*. *J. Biol. Chem.* **260**, 4637–4647 (1985).
22. D. R. Marous *et al.*, Consecutive radical S-adenosylmethionine methylations form the ethyl side chain in thienamycin biosynthesis. *Proc. Natl. Acad. Sci. U.S.A.* **112**, 10354–10358 (2015).
23. E. K. Sinner, M. S. Lichstrahl, R. Li, D. R. Marous, C. A. Townsend, Methylations in complex carbapenem biosynthesis are catalyzed by a single cobalamin-dependent radical S-adenosylmethionine enzyme. *Chem. Commun. (Camb.)* **55**, 14934–14937 (2019).
24. H. L. Knox, E. K. Sinner, C. A. Townsend, A. K. Boal, S. J. Booker, Structure of a B<sub>12</sub>-dependent radical SAM enzyme in carbapenem biosynthesis. *Nature* **602**, 343–348 (2022).
25. E. K. Sinner, C. A. Townsend, Purification and characterization of sequential cobalamin-dependent radical SAM methylases ThnK and TokK in carbapenem  $\beta$ -lactam antibiotic biosynthesis. *Methods Enzymol.* **669**, 29–44 (2022).
26. J. Bridwell-Rabb, A. Zhong, H. G. Sun, C. L. Drennan, H. W. Liu, A B<sub>12</sub>-dependent radical SAM enzyme involved in oxetanocin A biosynthesis. *Nature* **544**, 322–326 (2017).
27. A. Zhong, Y.-H. Lee, Y. N. Liu, H. W. Liu, Biosynthesis of oxetanocin-A includes a B<sub>12</sub>-dependent radical SAM enzyme that can catalyze both oxidative ring contraction and the demethylation of SAM. *Biochemistry* **60**, 537–546 (2021).
28. S. P. Gough, B. O. Petersen, J. O. Duus, Anaerobic chlorophyll isocyclic ring formation in *Rhodospirillum rubrum* requires a cobalamin cofactor. *Proc. Natl. Acad. Sci. U.S.A.* **97**, 6908–6913 (2000).
29. S. J. Booker, Anaerobic functionalization of unactivated C-H bonds. *Curr. Opin. Chem. Biol.* **13**, 58–73 (2009).
30. M. F. Freeman, K. A. Moshos, M. J. Bodner, R. Li, C. A. Townsend, Four enzymes define the incorporation of coenzyme A in thienamycin biosynthesis. *Proc. Natl. Acad. Sci. U.S.A.* **105**, 11128–11133 (2008).
31. M. Rodríguez *et al.*, Mutational analysis of the thienamycin biosynthetic gene cluster from *Streptomyces cattleya*. *Antimicrob. Agents Chemother.* **55**, 1638–1649 (2011).
32. D. A. Hopwood, T. Kieser, H. M. Wright, M. J. Bibb, Plasmids, recombination and chromosome mapping in *Streptomyces lividans* 66. *J. Gen. Microbiol.* **129**, 2257–2269 (1983).
33. A. Stapon, R. Li, C. A. Townsend, Carbapenem biosynthesis: Confirmation of stereochemical assignments and the role of CarC in the ring stereoinversion process from L-proline. *J. Am. Chem. Soc.* **125**, 8486–8493 (2003).
34. H. Aoki, H. Sakai, M. Kohsaka, T. Konomi, J. Hosoda, Nocardin A, a new monocyclic  $\beta$ -lactam antibiotic. I. Discovery, isolation and characterization. *J. Antibiot. (Tokyo)* **29**, 492–500 (1976).
35. N. D. Lanz *et al.*, Enhanced Solubilization of Class B Radical S-Adenosylmethionine Methylases by Improved Cobalamin Uptake in *Escherichia coli*. *Biochemistry* **57**, 1475–1490 (2018).
36. Y. Wang, B. Schnell, S. Baumann, R. Müller, T. P. Begley, Biosynthesis of branched alkoxy groups: Iterative methyl group alkylation by a cobalamin-dependent radical SAM enzyme. *J. Am. Chem. Soc.* **139**, 1742–1745 (2017).
37. N. Mahanta, D. Fedoseyenko, T. Dairi, T. P. Begley, Menaquinone biosynthesis: Formation of aminofutalosine requires a unique radical SAM enzyme. *J. Am. Chem. Soc.* **135**, 15318–15321 (2013).
38. L. E. Cooper *et al.*, In vitro reconstitution of the radical S-adenosylmethionine enzyme MqnC involved in the biosynthesis of futalosine-derived menaquinone. *Biochemistry* **52**, 4592–4594 (2013).
39. L. G. Ljungdahl, J. LeGall, J.-P. Lee, Isolation of a protein containing tightly bound 5-methoxybenzimidazolycobamide (factor 3m) from *Clostridium thermoaceticum*. *Biochemistry* **12**, 1802–1808 (1973).
40. H. G. Viehe, Z. Janousek, R. Merenyi, L. Stella, The captodative effect. *Acc. Chem. Res.* **18**, 148–154 (1985).
41. F. G. Bordwell, T. Y. Lynch, Radical stabilization energies and synergistic (captodative) effects. *J. Am. Chem. Soc.* **111**, 7558–7562 (1989).
42. J. Bridwell-Rabb, B. Li, C. L. Drennan, Cobalamin-dependent radical S-adenosylmethionine enzymes: Capitalizing on old motifs for new functions. *ACS Bio. Med. Chem. Au* **2**, 173–186 (2022).
43. J. C. Walton, Enhanced proton loss from neutral free radicals: Toward carbon-centered superacids. *J. Phys. Chem. A* **122**, 1422–1431 (2018).
44. K. Pius, J. Chandrasekar, Remarkably large captodative stabilisation in radical ions. *J. Chem. Soc. Chem. Commun.* **1**, 41–42 (1990).
45. J. T. Jarrett, The biosynthesis of thiol- and thioether-containing cofactors and secondary metabolites catalyzed by radical S-adenosylmethionine enzymes. *J. Biol. Chem.* **290**, 3972–3979 (2015).
46. C. J. Fugate, J. T. Jarrett, Biotin synthase: Insights into radical-mediated carbon-sulfur bond formation. *Biochim. Biophys. Acta* **1824**, 1213–1222 (2012).
47. M. M. Cosper *et al.*, Characterization of the cofactor composition of *Escherichia coli* biotin synthase. *Biochemistry* **43**, 2007–2021 (2004).
48. E. L. McCarthy, S. J. Booker, Destruction and reformation of an iron-sulfur cluster during catalysis by lipoyl synthase. *Science (80-)* **358**, 373–377 (2017).
49. R. M. Cicchillo *et al.*, Lipoyl synthase requires two equivalents of S-adenosyl-L-methionine to synthesize one equivalent of lipoic acid. *Biochemistry* **43**, 6378–6386 (2004).

50. R. M. Cicchillo *et al.*, *Escherichia coli* lipoyl synthase binds two distinct [4Fe-4S] clusters per polypeptide. *Biochemistry* **43**, 11770–11781 (2004).
51. K.-H. Lee *et al.*, Characterization of RimO, a new member of the methylthiotransferase subclass of the radical SAM superfamily. *Biochemistry* **48**, 10162–10174 (2009).
52. H. L. Hernández *et al.*, MiaB, a bifunctional radical-S-adenosylmethionine enzyme involved in the thiolation and methylation of tRNA, contains two essential [4Fe-4S] clusters. *Biochemistry* **46**, 5140–5147 (2007).
53. F. Forouhar *et al.*, Two Fe-S clusters catalyze sulfur insertion by radical-SAM methylthiotransferases. *Nat. Chem. Biol.* **9**, 333–338 (2013).
54. B. Zhang *et al.*, First step in catalysis of the radical S-adenosylmethionine methylthiotransferase MiaB yields an intermediate with a [3Fe-4S]<sup>0</sup>-like auxiliary cluster. *J. Am. Chem. Soc.* **142**, 1911–1924 (2020).
55. T. A. J. Grell, P. J. Goldman, C. L. Drennan, SPASM and twitch domains in S-adenosylmethionine (SAM) radical enzymes. *J. Biol. Chem.* **290**, 3964–3971 (2015).
56. K. L. Dunbar, D. H. Scharf, A. Litomska, C. Hertweck, Enzymatic carbon-sulfur bond formation in natural product biosynthesis. *Chem. Rev.* **117**, 5521–5577 (2017).
57. A. R. Balo, L. Tao, R. D. Britt, Characterizing SPASM/twitch domain-containing radical SAM enzymes by EPR spectroscopy. *Appl. Magn. Reson.* **53**, 809–820 (2022).
58. A. Benjdia, O. Berteau, Radical SAM enzymes and ribosomally-synthesized and post-translationally modified peptides: A growing importance in the microbiomes. *Front Chem.* **9**, 678068 (2021).
59. A. Benjdia *et al.*, Thioether bond formation by SPASM domain radical SAM enzymes: C<sub>α</sub> H-atom abstraction in subtilisin A biosynthesis. *Chem. Commun. (Camb.)* **52**, 6249–6252 (2016).
60. N. A. Bruender, V. Bandarian, B. Skf, SkfB abstracts a hydrogen atom from C<sub>α</sub> on SkfA to initiate thioether cross-link formation. *Biochemistry* **55**, 4131–4134 (2016).
61. C. Balty *et al.*, Biosynthesis of the sactipeptide Ruminococcin C by the human microbiome: Mechanistic insights into thioether bond formation by radical SAM enzymes. *J. Biol. Chem.* **295**, 16665–16677 (2020).
62. L. Flühe *et al.*, The radical SAM enzyme AlbA catalyzes thioether bond formation in subtilisin A. *Nat. Chem. Biol.* **8**, 350–357 (2012).
63. G. A. Hudson *et al.*, Bioinformatic mapping of radical S-adenosylmethionine-dependent ribosomally synthesized and post-translationally modified peptides identifies new C<sub>α</sub>, C<sub>β</sub>, and C<sub>γ</sub>-linked thioether-containing peptides. *J. Am. Chem. Soc.* **141**, 8228–8238 (2019).
64. R. B. Kapust *et al.*, Tobacco etch virus protease: Mechanism of autolysis and rational design of stable mutants with wild-type catalytic proficiency. *Protein Eng.* **14**, 993–1000 (2001).
65. A. J. Zehnder, K. Wuhmann, Titanium (III) citrate as a nontoxic oxidation-reduction buffering system for the culture of obligate anaerobes. *Science* **194**, 1165–1166 (1976).